

Numerical Study of Heat Transfer Enhancement with Nanofluid in Rectangular Duct.

AVIK RAY^{1*}, SUMANTA BANERJEE¹, PROKASH CHANDRA ROY²

¹Department of Mechanical Engineering, HITK, Kolkata, India

²Jadavpur University, Jadavpur, India

*Corresponding author's mail id: avik.ray@heritageit.edu

Abstract:

In order to reduce heat losses and enhance heat transfer efficiency, energy conservation and management in thermal systems has attracted interest on a global scale. Due to limitations on continuous improvement in thermophysical characteristics of traditional working fluids, R&D trends have shifted towards nanofluids applications in heat transfer systems. Literature review substantiates that single-particle nano fluids are well-suited for heat transfer applications. Employing hybrid nanofluids to improve heat transfer rates is a comparably new field of research and application.. In the present numerical study, enhancement of heat transfer rates is observed for flows of single-particle and hybrid nanofluids through a rectangular, straight duct of uniform cross-section, subjected to symmetrical and uniform wall heat flux conditions. The present work is carried out to investigate heat transfer augmentation characteristics of Al_2O_3/Cu hybrid nanofluids and Al_2O_3 single-particle nanofluids, for different nanoparticle mixture ratios dispersed in water. The simulations are performed with 0.5%, 1.0% and 2.0% volume fractions of nano particles. The Reynolds number of flow is varied from 2000 to 12000. The uniform heat flux applied along the tube length is $\approx 7955 \text{ W/m}^2$. The effects of Reynolds number, volume fraction, and composition of nanoparticles are analysed from the perspective of fluid and thermal analysis. The validation of the results obtained from present study has been performed with experimental and published data available in open literature. The wall-averaged Nusselt number and the pressure drop rise as the Reynolds number and the volume fraction is increased. This warrants a trade-off between heat transfer enhancement on one hand, and mechanical head losses on the other. The heat transfer characteristics of the chosen water- dispersed, hybrid nanofluid is also observed to be superior as compared to the single-particle nanofluid medium.

Keywords: Hybrid nanofluid; Single-particle nanofluid; Uniformly heated tube; Rectangular Channel; ANSYS

1. Introduction:

Advanced cooling techniques must be compact and, yet, highly effective in order to accommodate the ever-increasing needs of electronic equipment, and to ensure steady and reliable system operations [1]. Furthermore, the synthesis of energy-efficient heat transfer fluids, required for high-end and sophisticated cooling applications, is constrained by low values of thermal conductivity. Owing to restrictions on further advances in thermophysical properties of conventional fluids, state-of-art R&D trends have progressively switched to nanofluid applications in heat transfer systems [2]. Nowadays, techniques in nanotechnology enables production of metallic (or non-metallic) particles with \sim nm dimensions, with identical optical,

mechanical, electrical, magnetic, and thermal characteristics. Using adequate surfactants to prevent agglomeration, these nanoparticles (with average diameters \sim 100 nm) may be suspended steadily, and disseminated uniformly, in conventional heat transfer fluids (like water, oil, etc.).

A large body of published research have revealed how nanofluids affect heat transmission characteristics in forced convection through ducts (like circular or non-circular tubes). A brief survey of technical literature is presented in this context. A computational model, by Hussein et al. [3], enables to assess the heat transfer enhancement and friction factor for the flow of various types of nanofluids via tubes of three distinct forms (geometries), and have validated the same with experimental data

available in literature. Water-based nanofluid comprising of TiO_2 nanoparticles with volume fractions 1%, 1.5%, and 2.5% is used for three types of tubes (circular, elliptical and flat). The results indicate heat transfer augmentation as the volume fraction increases. For this study, a CFD model based on FVM has been used in FLUENT® environment. Experimental research on heat transfer by forced convection of TiO_2 /water nanofluids flowing in between a channel having varying cross sections has been done by Salimpour and D-Parizi [4]. According to their findings, nanofluids enhance the heat transfer for flow through conduits. Moreover, experimental studies reveal that conduits with circular cross section perform better than square and triangular cross sections conduits in terms of heat transfer performance. Hwang et al. [5] have calculated the heat transfer coefficient and pressure reduction of water-based Al_2O_3 nanofluids passing through a circular duct, considering homogeneous wall heat flux under the laminar flow regime. As compared with water, the heat transfer enhancement is observed to be ~8% at a volume fraction of ~0.3 vol%. The improvement in convective heat transfer coefficient exceeds the rise in thermal conductivity, by a wide margin. This finding provides perfect stimulus for further studies on heat transfer enhancement in other generic systems using nanofluids. Based on scale analysis and numerical simulations, the study describes how rapid changes in bulk properties like nanoparticle concentration, thermal conductivity, and viscosity influence steady-state velocity profiles. The heat transfer coefficient significantly rises, owing to resultant temperature gradients that are intricately coupled with the velocity field. Aminian et al. [6] have conducted a computational study on the influence of magnetic field on the laminar flow of Al_2O_3/CuO –water hybrid nanofluid filled inside a segmented cylinder in a porous medium, where the cylinder walls are exposed to a uniform heat flux. The computations have been done for a wide variety of governing factors. The impacts of the Hartmann number, Darcy number and the magnetic field on heat transmission and pressure drop have been studied. The aforementioned survey of literature provides an overview of the analytical, experimental, and/or computational investigations that are primarily focused on flow and heat transfer studies of primarily single-particle nanofluid systems. However, open research literature on heat transfer using hybrid nanofluids as the working medium are relatively few. In addition, studies on internal convection through rectangular ducts have been barely reported, although pipes of rectangular cross-sections are routinely used in solar collectors, heat exchangers, etc. The present numerical study aims to compare the different flow and heat-transfer parameters

($h, Nu, \Delta P, f$) for water, single-particle Al_2O_3 , and hybrid Al_2O_3/Cu nanofluids in a straight tube geometry of rectangular cross-section. The investigations are performed for different values of the Reynolds number and volume fractions of nanoparticles (for both the single-particle and hybrid grades). From heat transfer point of view, the primal outcome from this study is a comparison of performance of a hybrid nanofluid synthesized by mixing two nanoparticles, one Al_2O_3 (which offers greater stability and lower thermal conductivity) and the other Cu (which offers lesser stability and higher thermal conductivity), for varying nanoparticle volume fractions.

Nomenclature:

| | | | | | |
|-----------|------------------------------------------------------|------------------|-------------------------|-------|------------------|
| C | Specific heat capacity [J/kgK] | V | Volume [m^3] | bf | Base fluid |
| D | Hydraulic Diameter [m] | ρ | Density [kg/m^3] | hnf | Hybrid nanofluid |
| \bar{f} | Friction factor | μ | Viscosity [$Pa.s$] | $np1$ | Nano particle 1 |
| h | Convective heat transfer coefficient [W/m^2K] | φ | Volume fraction | $np2$ | Nano particle 2 |
| k | Thermal conductivity [W/mK] | <i>Subscript</i> | | | |
| N | Nusselt number | np | Nano particle | | |
| P | Pressure [N/m^2] | nf | Nanofluid | | |

2. Measurements of Thermophysical Properties

Table 1 show the properties of the base fluid water and the considered nanoparticles (Al_2O_3, Cu). The nano particles have a spherical form with ~100 nm size. All of these properties have been modeled as temperature-independent [7].

Table 1. Properties of using different elements.

| Property | Water | Al_2O_3 | Cu |
|----------|-------|-----------|------|
| ρ | 998.2 | 3970 | 8300 |
| C | 4182 | 765 | 420 |
| k | 0.6 | 40 | 401 |
| μ | 0.001 | - | - |

2.1 Properties of Single particle nanofluid

Commonly-used models from published research literature have been utilised to estimate the thermophysical characteristics of single-particle

and hybrid nanofluids [8, 9]. The volume fraction is expressed as follows [8, 10]:

$$\phi = \frac{V_{np}}{V_{bf} + V_{np}} \quad (1)$$

Eq. (1) relates ϕ with the volume of the basefluid (V_{bf}) and the volume of the nanoparticles ($V_{np} = m_{np}/\rho_{np}$), where m_{np} is the nano particle mass.

$$\rho_{nf} = (1 - \phi)\rho_{bf} + \phi\rho_{np} \quad (2)$$

In Eq. (2), calculating the density of a nanofluid involves taking into account its base fluid density (ρ_{nf}), volume fraction (ϕ), and nanoparticle density (ρ_{np}). The following equation (Eq. (3)) calculates the specific heat ($C_{p,nf}$) of nanofluid in terms of specific heat ($C_{p,bf}$) of basefluid and specific heat ($C_{p,np}$) of nanoparticles:

$$C_{p,nf} = \frac{(1-\phi)\rho_{bf}C_{p,bf} + \phi\rho_{np}C_{p,np}}{\rho_{nf}} \quad (3)$$

In Eq. (4) below, the effective thermal conductivity (k_{nf}) of the nanofluid is calculated in terms of thermal conductivity (k_{bf}) of basefluid and thermal conductivity (k_{np}) of nanoparticles:

$$k_{nf} = k_{bf} \left[\frac{(k_{np} + 2k_{bf}) - 2\phi(k_{bf} - k_{np})}{(k_{np} + 2k_{bf}) + \phi(k_{bf} - k_{np})} \right] \quad (4)$$

Eq. (5) evaluates the effective dynamic viscosity (μ_{nf}) of the nanofluid in terms of volume fraction and the viscosity (μ_{bf}) of base fluid:

$$\mu_{nf} = \frac{\mu_{bf}}{(1-\phi)^{2.5}} \quad (5)$$

2.2 Hybrid nanofluid properties

The volume fraction of the hybrid nanofluid is expressed as the sum of the volume fractions of the respective components [9]:

$$\phi_{hnf} = \phi_{np1} + \phi_{np2} \quad (6)$$

Once ϕ_{hnf} is calculated from Eq. (6), the density of the hybrid nanofluid (ρ_{hnf}) can be evaluated from the volume fractions (ϕ_{np1}, ϕ_{np2}) and density values (ρ_{np1}, ρ_{np2}) of the constituent nanoparticles, and the base fluid density (ρ_{bf}), as seen from Eq. (7):

$$\rho_{hnf} = \phi_{np1}\rho_{np1} + \phi_{np2}\rho_{np2} + (1 - \phi_{hnf})\rho_{bf} \quad (7)$$

The specific heat of hybrid nanofluid ($C_{p,hnf}$) can be expressed in terms of the specific heats of

nanoparticles ($C_{p,np1}, C_{p,np2}$), and the specific heat ($C_{p,bf}$) of the base fluid (see Eq. (8) below):

$$C_{p,hnf} = \frac{\phi_{np1}\rho_{np1}C_{p,np1} + \phi_{np2}\rho_{np2}C_{p,np2} + (1 - \phi_{hnf})\rho_{bf}C_{p,bf}}{\rho_{hnf}} \quad (8)$$

The effective thermal conductivity of the hybrid nanofluid (k_{hnf}) can now be calculated, in terms of the volume fractions (ϕ_{np1}, ϕ_{np2}) and the thermal conductivities of the constituent nanoparticles (k_{np1}, k_{np2}) and the base fluid (k_{bf}):

$$k_{hnf} = \frac{\phi_{np1}k_{np1} + \phi_{np2}k_{np2} + 2k_{bf} + 2(\phi_{np1}k_{np1} + \phi_{np2}k_{np2}) - 2\phi_{hnf}k_{bf}}{\phi_{hnf}} \quad (9)$$

Lastly, Eq. (10) enables to compute the effective viscosity of hybrid nanofluid (μ_{hnf}) is computed in terms of the viscosity of the base fluid (μ_{bf}), as well as the volume fractions of the constituent nanoparticles 1 and 2:

$$\mu_{hnf} = \mu_{bf} \frac{1}{(1 - \phi_{np1} - \phi_{np2})^{2.5}} \quad (10)$$

3. Problem Description and Mathematical Model

The 3D computational region of the physical system is depicted in Fig. 1. The annular channel, made of copper, has a length is 1500 mm. The inner square has sides of 16 mm, and the outer square has side measuring 19 mm [10]. Considering constant wall heat-flux conditions, a copper conduit using water, single-particle, and hybrid nanofluids as working substances is explored using computational fluid dynamics (CFD) techniques. The main objective of this study is to find out the fluid flow and heat transfer characteristics in the channel. Keeping the same heat input rate, the (calculated) value of heat flux for the present configuration is $\approx 7955 \text{ W/m}^2$

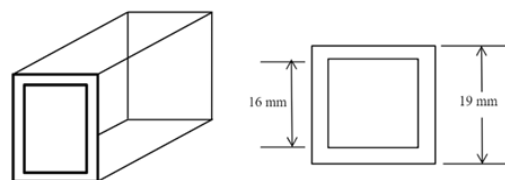


Fig. 1: Configuration of 3D channel

Considering flow of various working fluids, the conservation equations of mass, momentum and energy are solved for the chosen channel configuration to simulate thermal and flow characteristics [11].

Continuity Equation:

$$\nabla \cdot (\rho \vec{V}) = 0 \quad (11)$$

Momentum Equation:

$$\nabla \cdot (\rho \vec{V} \vec{V}) = -\nabla P + \nabla \cdot \tilde{\tau} \quad (12)$$

Energy Equation:

$$\nabla \cdot (\rho \vec{V} h) = \nabla \cdot (k \nabla T) + \tilde{\tau} : \nabla \vec{V} \quad (13)$$

The stress tensor $\tilde{\tau}$ (Eq. (12) and Eq. (13)) is expressed in terms of velocity field \vec{V} (δ is the Kronecker delta):

$$\tilde{\tau} = \mu \left[\nabla \vec{V} + (\nabla \vec{V})^T - \frac{2}{3} \delta (\nabla \cdot \vec{V}) \right] \quad (14)$$

In Eqs. (11)-(14) P is the pressure field and h the specific enthalpy. The $k - \epsilon$ turbulence model has also been incorporated in the numerical analysis in line with [8]. Here k & ϵ are the turbulent kinetic energy and turbulent dissipation rates respectively.

The simulations are carried out using a solution based on the Finite Volume Method, assuming the flow is uniform, stable, and incompressible [9]. The SIMPLE algorithm is used for the solution of the conservation equations, and the convection-diffusion terms are discretized using the Power Law technique [12]. As mentioned, the $k - \epsilon$ model for turbulent viscosity has been used. The convergence criteria for all the field equations have been set at $\sim 10^{-8}$. The boundary conditions are uniform heat flux ($\approx 7955 \text{ W/m}^2$) applied to walls of the channel with symmetrical distribution [10]. The inlet velocity, with different values of the Reynolds number for working fluids, and the pressure outlet conditions are provided and the inlet fluid temperature is $\approx 298.15 \text{ K}$. The working fluids considered are water, single-particle (Al_2O_3) and hybrid (Al_2O_3/Cu (1:1)) –water nanofluid.

4. Evaluation of Different Parameters

The average heat transfer coefficient ($= \bar{h}$) is estimated considering rate of heat transfer ($= \dot{Q}$), heat transfer area ($= A$), mean surface temperature of the wall ($= T_s$) and mean temperature of fluid ($= T_b$) [13, 14]:

$$\bar{h} = \dot{Q} / A (T_s - T_b) \quad (15)$$

Given the rate of mass flow ($= \dot{m}_f$) of fluid and the computed values of the fluid mean temperatures at the inlet ($= T_{b,i}$) and the exit ($= T_{b,o}$) sections, the heat transfer rate ($= \dot{Q}$) by the working fluid is evaluated as:

$$\dot{Q} = \dot{m}_f c_p (T_{b,o} - T_{b,i}) \quad (16)$$

The mean Nusselt number ($= \overline{Nu}$) is evaluated considering the hydraulic diameter ($= D$) of the rectangular duct:

$$\overline{Nu} = \bar{h} D / k_f \quad (17)$$

The average friction factor (\bar{f}) is calculated by the pressure drop ($= \Delta P$), length of the channel ($= L$), hydraulic diameter, fluid density and the mean velocity ($= \bar{U}$):

$$\bar{f} = \frac{\Delta P}{\left(\frac{L}{D}\right) \left(\frac{\rho \bar{U}^2}{2}\right)} \quad (18)$$

In Eq. (19), the pressure drop is expressed as the difference of the inlet and outlet fluid pressures:

$$\Delta P = P_{f,i} - P_{f,o} \quad (19)$$

$$P_p = \bar{U} A \Delta P \quad (20)$$

In Eq. (20), the pumping power (P_p) is expressed, where A is the cross-sectional area of the duct.

4.1 Grid independence test

Five alternative mesh element counts, from 10^5 to 7×10^5 , have been used to confirm grid independence. Figures 2(a) and 2(b) show how the Nusselt number (Nu) and the average friction factor (f) change as the number of mesh elements rises. The variation trends indicate that across the grid item amount of 555291, the marginal changes in the values of Nu and f are in the range of $\sim 2\%$. Due to this, a total of 555291 mesh elements were chosen for the study.

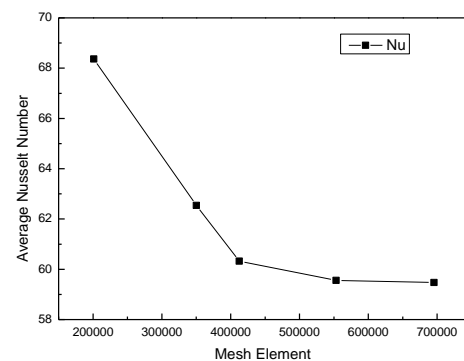


Fig. 2(a): Average Nusselt number versus mesh elements

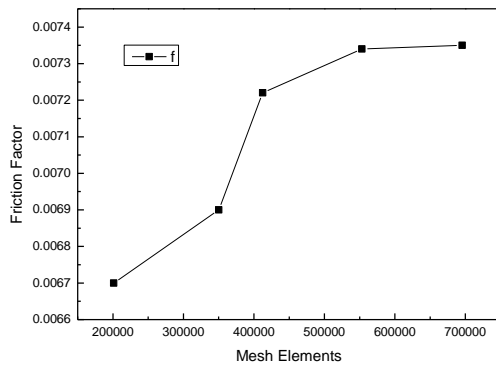


Fig. 2(b): Friction factor versus mesh elements number

5. Results and Discussions:

5.1. Validation

The experimental data for the circular tube configuration, for the identical set of temperature and pressure boundary conditions, have been employed to validate the mathematical model based on CFD methodologies [10]. This is illustrated in Fig 3a & Fig 3b. The mean difference across the experimental and the computational values of the Nusselt number and friction factor (for all Reynolds number variations examined) is $\sim 7.89\%$ and $\sim 8.55\%$, respectively.

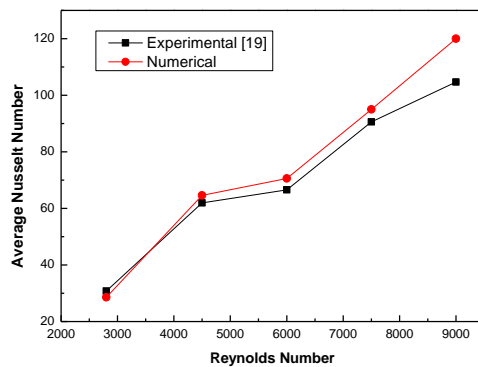


Fig. 3(a): Average Nusselt number versus Re

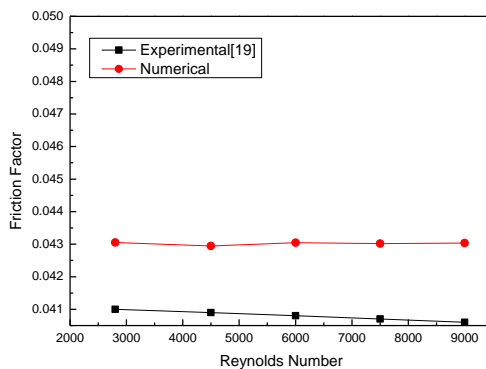


Fig. 3(b): f versus Re

5.2. Properties of Nanofluid

The calculated values of nanofluid thermophysical properties (putting $\phi_{nmf} = 0.02$; $\phi_{nv1} = 0.01$; $\phi_{nv2} = 0.01$ in Eq. (6) – Eq. (10)) are listed in Table 2. For the hybrid Al_2O_3/Cu nanofluid, the nanoparticles are mixed in the same proportion (i.e. 50/50 %).

Table 2: Properties of Nanofluids [as calculated by Eq. (6) – Eq. (10)]

| Nanofluid | Density (kg/m^3) | Specific Heat (J/kgK) | Thermal Conductivity (W/mK) | Viscosity ($Pa.s$) |
|-------------------|----------------------|---------------------------|---------------------------------|----------------------|
| 0.5% Al_2O_3 | 1013.059 | 4115.047 | 0.6086 | 0.001013 |
| 0.5% Al_2O_3/Cu | 1023.884 | 4072.637 | 0.612 | 0.001013 |
| 1% Al_2O_3 | 1027.918 | 4050.029 | 0.617 | 0.001025 |
| 1% Al_2O_3/Cu | 1049.568 | 3968.626 | 0.624 | 0.001025 |
| 2% Al_2O_3 | 1057.636 | 3925.475 | 0.635 | 0.001052 |
| 2% Al_2O_3/Cu | 1100.936 | 3775.164 | 0.649 | 0.001052 |

5.3. Nusselt Number

Figure 4 illustrates that the Nu changes as the Re rises for various using fluids. The Nusselt number rises as the volume concentration and turbulence level rise. The hybrid-grade Al_2O_3/Cu nanofluid presents a better performance in heat transfer enhancement, as compared to Al_2O_3 nanofluid due to its higher thermal conductivity. It's observed that the average Nusselt numbers ($= \overline{Nu}$) of Al_2O_3 nanofluid are respectively higher by $\approx 2.7\%$, $\approx 5.2\%$ and $\approx 10.9\%$ at nano particle volume fraction from 0.5%, 1.0% and 2.0% respectively; whereas 4.1%, $\approx 8.0\%$ and $\approx 16.2\%$ Nusselt Number enhancement observed for hybrid nanofluid in contrast with water. 3 times Nusselt number increases of 2% hybrid nanofluid, when Reynolds number increases from 2000 to 12000. As an end result heat from the system is eliminated the fastest when 2% hybrid nanofluid is used.

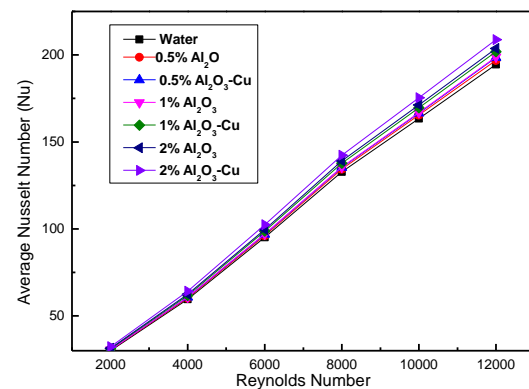


Fig. 4: Plots of average wall Nu versus Re

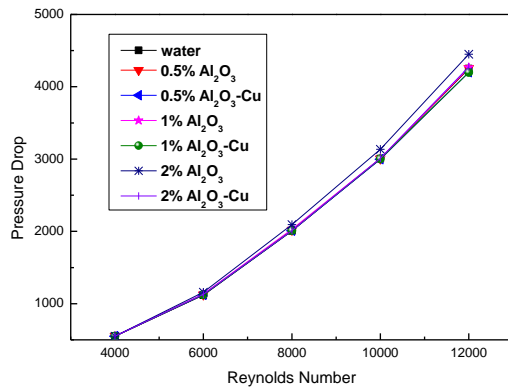


Fig. 5: Pressure drop versus Re for various working fluid

5.4. Pressure Drop

The pressure decrease of water, Al_2O_3 and Al_2O_3/Cu with various volume percentages and Reynolds numbers is depicted in Fig. 5. For all fluids, pressure loss rises as the Re increases due to an increase in turbulence intensity [15]. The pressure drop for both the nanofluids are superior to water, owing to higher values of effective viscosity coefficients. For the chosen set of flow conditions, 2% Al_2O_3 shows the highest pressure drop compared to others working fluids. Higher pressure drop is the drawback of employing nano fluids in the system. This is because of its required higher pumping power to sustain the flow.

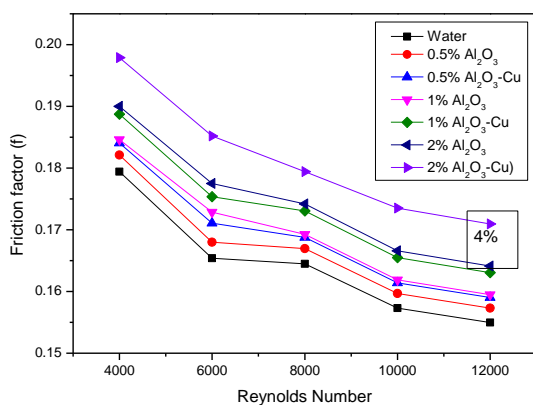


Fig. 6: Friction factor versus Reynolds number for various working fluids

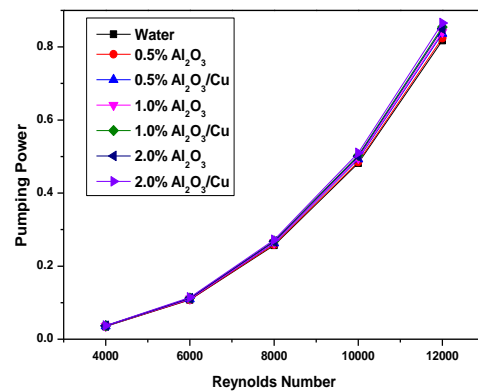


Fig. 7: Pumping Power versus Reynolds number for various working fluids

5.5. Friction factor

Effect of varying volume fraction (0.5% - 2%) ranges on friction factor is illustrated in Fig. 6. The results reveal that the friction factor reduces with increasing Reynolds number for any amount of disperse particle concentration [13, 16]. However, for any given Reynolds number, single and hybrid nanofluids have a larger friction factor than water. This is due to the increased viscosity of nanofluid in comparison to water. When the wall-averaged friction factor values for hybrid and single particle nanofluids at 2% volume fraction are compared, a larger increase of \bar{f} ($\approx 4\%$) is seen. Although a hybrid nanofluid with a 2% volume fraction enhances heat transfer rate (as compared to a single particle nanofluid having 2% volume fraction), it has the disadvantage of increasing friction loss. This is not acceptable. The friction factor increases by around 1% and 2.3% for 0.5% and 1% volume fractions, respectively. At low volume fractions, the system is shown to be cooled by hybrid nanofluid without a detectable increase in frictional loss.

5.6 Pumping Power

Pumping power is linked to pressure drop, rate of flow, and closed tube shape. Fig. 7 depicts the relationship between pumping power and Reynolds number. The pumping power increases fast as Re increases. Pumping power, like pressure drop, is lowest for water and increases with nano particle volume percentage, reaching maximum values for 2% Hybrid nanofluid.

Conclusions:

In this study, a CFD analysis has been conducted in ANSYS®/FLUENT® environment to investigate the effects of Al_2O_3 –water and hybrid

nanofluid (Al_2O_3/Cu) flow on heat transfer and pressure drop within a rectangular duct. According to the study,

- (a) The values of the average heat transfer coefficient (and, consequently, the average Nu climb for both nanofluids ($Al_2O_3, Al_2O_3/Cu$) as the Reynolds number and volume fraction of nanoparticles rise. Nanofluids containing 2.0 % Al_2O_3 and Al_2O_3/Cu exhibit heat transfer coefficients that are $\approx 10\%$ and $\approx 16\%$ greater than water, respectively.
- (b) However, pressure drop exhibit growing trend and friction factor decreases by increasing values of Re .
- (c) Even while a hybrid nanofluid with a 2% volume fraction will improve heat transfer rates (relative to a single particle nanofluid with a 2% volume fraction), this will result in increased friction loss more power required to maintain the flow. This is not desired.

References:

- [1] Dadhich M, Prajapati OS, Sharma V. Investigation of boiling heat transfer of titania nanofluid flowing through horizontal tube and optimization of results utilizing the desirability function approach. *Powder Technology*. 2021 Jan 22; 378:104-23.
- [2] Sheikh NA, Chuan Ching DL, Khan I. A comprehensive review on theoretical aspects of nanofluids: Exact solutions and analysis. *Symmetry*. 2020 May 3;12(5):725.
- [3] Hussein AM, Sharma KV, Bakar RA, Kadrigama K. The effect of cross sectional area of tube on friction factor and heat transfer nanofluid turbulent flow. *International Communications in Heat and Mass Transfer*. 2013 Oct 1; 47:49-55.
- [4] Salimpour MR, Dehshiri-Parizi A. Convective heat transfer of nanofluid flow through conduits with different cross-sectional shapes. *Journal of Mechanical Science and Technology*. 2015 Feb; 29(2):707-13.
- [5] Hwang KS, Jang SP, Choi SU. Flow and convective heat transfer characteristics of water-based Al_2O_3 nanofluids in fully developed laminar flow regime. *International journal of heat and mass transfer*. 2009 Jan 15; 52(1-2):193-9..
- [6] Aminian E, Moghadasi H, Saffari H. Magnetic field effects on forced convection flow of a hybrid nanofluid in a cylinder filled with porous media: A numerical study. *Journal of Thermal Analysis and Calorimetry*. 2020 Sep; 141(5):2019-31.
- [7] Chaurasia SR, Sarviya RM. Comparative thermal performance analysis with entropy generation on helical screw insert in tube with number of strips with nanofluid at laminar flow regime. *International Communications in Heat and Mass Transfer*. 2021 Mar 1; 122:105138.
- [8] Garud KS, Lee MY. Numerical Investigations on Heat Transfer Characteristics of Single Particle and Hybrid Nanofluids in Uniformly Heated Tube. *Symmetry*. 2021 May 14;13(5):876.
- [9] Sanches M, Marseglia G, Ribeiro AP, Moreira AL, Moita AS. Nanofluids characterization for spray cooling applications. *Symmetry*. 2021 May 2; 13(5):788.
- [10] Lee MY, Seo JH, Lee HS, Garud KS. Power generation, efficiency and thermal stress of thermoelectric module with leg geometry, material, segmentation and two-stage arrangement. *Symmetry*. 2020 May; 12(5):786.
- [11] Ghasemi SE, Ranjbar AA, Hosseini MJ. Numerical study on effect of CuO-water nanofluid on cooling performance of two different cross-sectional heat sinks. *Advanced Powder Technology*. 2017 Jun 1; 28(6):1495-504.
- [12] S.V. Patankar, *Numerical Heat Transfer and Fluid Flow*, McGraw-Hill, New York, 1981
- [13] Nabi H, Pourfallah M, Gholinia M, Jahanian O. Increasing heat transfer in flat plate solar collectors using various forms of turbulence-inducing elements and CNTs-CuO hybrid nanofluids. *Case Studies in Thermal Engineering*. 2022 May 1; 33:101909.
- [14] Kristiawan B, Rifa'i AI, Enoki K, Wijayanta AT, Miyazaki T. Enhancing the thermal performance of TiO_2 /water nanofluids flowing in a helical microfin tube. *Powder Technology*. 2020 Oct 1; 376:254-62.
- [15] Kristiawan B, Rifa'i AI, Enoki K, Wijayanta AT, Miyazaki T. Enhancing the thermal performance of TiO_2 /water

nanofluids flowing in a helical microfin tube. Powder Technology. 2020 Oct 1; 376:254-62.

- [16] Ghasemi SE, Ranjbar AA, Hosseini MJ. Numerical study on effect of CuO-water nanofluid on cooling performance of two different cross-sectional heat sinks. Advanced Powder Technology. 2017 June; 28: 1495-1504.